Cement and Concrete Research 42 (2012) 982–993

Contents lists available at SciVerse ScienceDirect

Cement and Concrete Research

journal homepage: http://ees.elsevier.com/CEMCON/default.asp

Nucleation and growth models for hydration of cement

George W. Scherer [a,*], Jie Zhang [a,1], Jeffrey J. Thomas [b]

[a] Princeton University, Civil & Env. Eng., Eng. Quad. E-319, Princeton, NJ 08544, USA
[b] Schlumberger-Doll Research, Cambridge, MA 02139, USA

ARTICLE INFO

Article history:
Received 24 November 2011
Accepted 27 March 2012

Keywords:
Kinetics (A)
Hydration (A)
Calorimetry (A)
Shrinkage (C)

ABSTRACT

The hydration of cement is often modeled as a nucleation and growth process. In this paper, we examine the applicability of the boundary nucleation and growth model, in which nucleation is assumed to occur only on the surfaces of the cement particles. This theory has been shown to give good fits to calorimetric and chemical shrinkage data, with the assumption that the nucleation and growth rates are constant. However, we will show that slightly better fits are obtained when it is assumed that growth occurs from a fixed number of nuclei. We present a version of the model that allows for anisotropic growth, with different rates on each side of the particle surface. This type of model must only be used during the period when the reaction is dominated by a single phase, but this is approximately valid during the time when the paste is setting.

1. Introduction

Extensive research has been devoted to the hydration reaction of ordinary Portland cement and its component oxides (particularly, C_3S and C_2S).[2] This work has been discussed in comprehensive books and reviews [*e.g.*, 1–4]. It is widely accepted that the early stage of hydration, including the time of initial and final setting of a paste, involves a mechanism of nucleation and growth of hydration product. This idea is supported by the good performance of analytical models based on that idea [*e.g.*, 5–9], and the results of simulations based on fundamental reaction models [10,11]. Recently, Thomas [9] pointed out that the conventional Johnson–Mehl–Avrami–Kolmogorov (JMAK) model [12–14], which assumes that nuclei are randomly distributed throughout the reaction volume, is not appropriate for describing the hydration reaction, where nucleation occurs primarily on the surface of the cement particles. Instead, he applied a model that was developed by Cahn [15] to describe transformations in polycrystalline materials, where nucleation occurs on grain boundaries. This model (hereafter called BNG = boundary nucleation and growth) was found to give an improved fit to calorimetric data for hydration of C_3S [9], under the assumptions that the rates of nucleation (per unit area of exposed clinker surface) and growth are constant throughout the process. However, computer simulations indicate that the evolution of the solution composition is such that a burst of nucleation is expected in the first few minutes of hydration, after which a stable supersaturation is maintained [10,11]. Under these conditions, growth would be expected to occur from a fixed number of nuclei.

The purpose of this paper is to extend the BNG model to allow for anisotropic growth from a constant number of nuclei or with a constant rate of nucleation. As noted by Taylor [Ref. 1, p. 223], the observed kinetics is the sum of the rates for all the phases undergoing reaction, so we will consider how the model should be applied to Portland cement, where the hydration of several phases is concurrent.

The theoretical development is presented in the next section. In Section 2.1, we show how the volume fraction of product, which is calculated from the nucleation and growth model, is related to the degree of hydration and the chemical shrinkage. In Sections 2.2 and 2.3, we will derive the transformation rate when nucleation occurs at a constant rate or from a constant number of nuclei, respectively. Since nucleation is assumed to occur only on the portion of the surface of the clinker that is not yet covered with hydration products, the rate of production of nuclei drops to zero as the hydrates spread across the surfaces of the cement particles. Therefore, although the rate of nucleation per unit area of exposed surface is constant, the net rate of nucleation drops, and the transformation rates tend to converge for systems having a constant number of nuclei or a constant nucleation rate. Section 2.4 describes the situation where multiple phases are reacting. In Section 3, the model is compared to chemical shrinkage data for Class H cement, and it is demonstrated that the results are slightly better when growth is assumed to occur from a fixed number of nuclei. The implications of these results are discussed in Section 4.

* Corresponding author. Tel.: +1 609 258 5680.
E-mail address: scherer@princeton.edu (G.W. Scherer).
[1] Present address: University of Michigan, Civil & Env. Eng., 2314 GG Brown Building, Ann Arbor, MI 48105, USA.
[2] We use standard cement chemistry notation: C = CaO, S = SiO_2, A = Al_2O_3, F = Fe_2O_3, H = H_2O.

0008-8846/$ – see front matter © 2012 Elsevier Ltd. All rights reserved.
doi:10.1016/j.cemconres.2012.03.019

2. Theory

2.1. Relating volume fraction, degree of hydration, and chemical shrinkage

Nucleation and growth models predict the volume fraction, X, of the system that has been converted to the product phase; however, the quantity that is directly measured may be the heat released [9], water consumed [6–8], or chemical shrinkage [16]. Therefore, it is useful to provide an explicit connection between X and the degree of reaction, α, and the chemical shrinkage, s. Suppose that a volume of water, V_w, is mixed with a volume of cement, V_c, to make a paste. The water/cement mass ratio, R_{wc} (interchangeably written as w/c), is

$$R_{wc} = \frac{V_w \rho_w}{V_c \rho_c} \tag{1}$$

where ρ_w and ρ_c are the densities of water and cement, respectively. Now suppose that the hydration reaction consumes masses m_w of water and m_c of cement to make mass m_H of hydration products (including all product phases):

$$m_w + m_c = m_H. \tag{2}$$

The volume change on hydration is

$$\Delta V_H = \frac{m_H}{\rho_H} - \frac{m_w}{\rho_w} - \frac{m_c}{\rho_c} = m_c\left(\frac{1}{\rho_H} - \frac{1}{\rho_c}\right) + m_w\left(\frac{1}{\rho_H} - \frac{1}{\rho_w}\right) \tag{3}$$

where ρ_H is the average density of the ensemble of solid hydration products. As hydration proceeds, and the species undergoing hydration change (from predominantly C_3S to C_2S), ρ_H will change; however, we are primarily interested in the early stage of hydration, so we will ignore this complication. If the hydration product consists of needles or sheets with liquid water between them, that water does not affect the value of ρ_H, although it contributes to the volume permeated by hydration products.

The chemical shrinkage, s, is reported as ΔV_H per gram of the original cement, so

$$s = \frac{\Delta V_H}{V_c \rho_c}. \tag{4}$$

The degree of hydration, α, is defined as the fraction of the original cement that has been consumed in the hydration reaction, so

$$\alpha = \frac{m_c}{V_c \rho_c}. \tag{5}$$

Experiments (see Fig. 1) indicate that the ratio between s and α is approximately constant:

$$c \equiv \frac{s}{\alpha} \approx \frac{\Delta V_H}{m_c} = \left(\frac{m_w}{m_c}\right)\left(\frac{1}{\rho_H} - \frac{1}{\rho_w}\right) + \frac{1}{\rho_H} - \frac{1}{\rho_c}. \tag{6}$$

When hydration is complete, $\alpha \to 1$, so $m_c \to V_c \rho_c$ and $s \to c$. Rearranging Eq. (6) indicates that the average water/cement ratio of the ensemble of hydration products is

$$\frac{m_w}{m_c} = \frac{c + 1/\rho_c - 1/\rho_H}{1/\rho_H - 1/\rho_w}. \tag{7}$$

Let us assume, as an upper bound on the density of the product, that ρ_H can be approximated by the density of saturated C-S-H, which Jennings reports to be 2.23 g/cm^3 [17]. Given $\rho_c = 3.22$ g/cm^3 [16], $\rho_w = 1.0$ g/cm^3, and $c = -0.0764$ cm^3/g (from the slope in Fig. 1 corresponding to 25 °C), Eq. (7) indicates that $m_w/m_c \approx 0.39$. The results in Fig. 1 indicate that the chemical shrinkage at a given degree of hydration decreases with increasing temperature. If we assume that the stoichiometry is constant, this implies a decrease in the skeletal density of the hydration products as T increases. The latter trend has been reported in several experimental studies, including Refs. [16,18,20] (where it is discussed at length). Bishnoi and Scrivener [24] assume that $\rho_H \approx 2.0$ g/cm^3, Garrault et al. [19] conclude that the earliest hydration product has $\rho_H \approx 2.1$ g/cm^3 and Thomas et al. [20] find a density of 2.05 g/cm^3 for saturated C-S-H. Using the latter value, Eq. (7) yields $m_w/m_c \approx 0.50$ at 25 °C. The densities and stoichiometries found for these limiting cases are shown in Table 1.

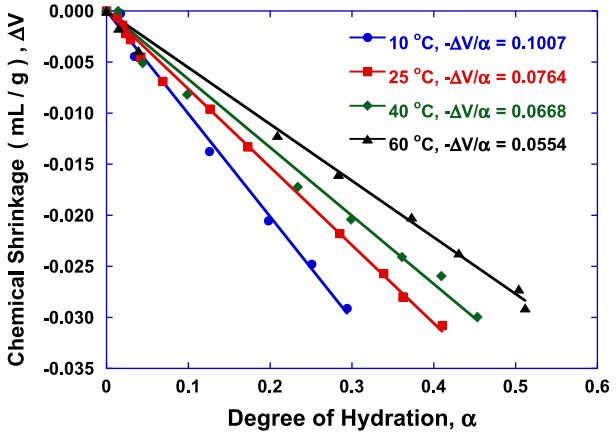

Fig. 1. Chemical shrinkage *versus* degree of hydration for Class H cement hydrated at w/c = 0.35 for up to 3 days.
Data from Ref. [16].

The nucleation and growth models calculate the volume occupied by hydrates, m_H/ρ_H, normalized by the *initial* volume of the body, $V_w + V_c$; that is, the volume change during the reaction is ignored:

$$X = \frac{m_H/\rho_H}{V_w + V_c}. \tag{8}$$

Eq. (8) is based on the assumption that the hydration products constitute a compact mass with a density of ρ_H. In the BNG models, it is further assumed that when two such masses impinge on one another, growth normal to the plane of contact must stop. Suppose, however, that the hydration product is a mass of needles, sheets, and other structures with liquid water in the interstices. If the volume fraction of solids in that mass is ϕ, then the total volume occupied by the products is found by dividing the right side of Eq. (8) by ϕ. However, when two such porous masses impinge, some interpenetration might be possible. In that case, the effect of impingement on the subsequent rate of growth of the product would not correctly be predicted by the standard BNG models. This point will be reconsidered in the Discussion; for the present, we ignore the existence of interstitial water, and base the analysis on Eq. (8).

Table 1
Stoichiometry and density (g/cm^3) of hydrates from Eq. (7).

T (°C)	c (ml/g)	ρ_H (g/cm^3) if m_w/m_c=		m_w/m_c if ρ_H (g/cm^3)=		$B = \alpha/X$ if m_w/m_c=	
		0.39	0.50	2.23	2.05	0.39	0.50
10	−0.1007	2.32	2.12	0.43	0.54	1.10	0.94
25	−0.0764	2.23	2.05	0.39	0.50	1.06	0.91
40	−0.0668	2.20	2.02	0.37	0.48	1.04	0.89
60	−0.0554	2.16	1.99	0.35	0.42	1.03	0.88

Using Eqs. (1)–(7), we obtain

$$\frac{X}{\alpha}=\left(\frac{\rho_c/\rho_H}{R_{wc}\rho_c/\rho_w+1}\right)\left(\frac{c+1/\rho_c-1/\rho_H}{1/\rho_H-1/\rho_w}\right)\equiv\frac{1}{B} \tag{9}$$

and

$$\frac{X}{s}=\left(\frac{1}{c}\right)\left(\frac{\rho_c/\rho_H}{R_{wc}\rho_c/\rho_w+1}\right)\left(\frac{c+1/\rho_c-1/\rho_H}{1/\rho_H-1/\rho_w}\right)\equiv\frac{1}{A}. \tag{10}$$

The quantity A defined in Eq. (10) is a constant (unless ρ_H changes during the course of hydration), so the shrinkage is proportional to X, and $s\to A$ as $X\to 1$. Using $c=-0.0764\ \mathrm{cm^3/g}$ (for $T=25\ ^\circ\mathrm{C}$), $\rho_H\approx 2.23\ \mathrm{g/cm^3}$, and $R_{wc}=0.35$, Eq. (10) yields $A\approx -0.081$. Using the same parameters, the ratio of α to X from Eq. (9) is given in Table 1. If a paste is prepared with a low w/c, the original water-filled space fills with hydration products and the reaction effectively stops while $X<1$ (*i.e.*, while some of the volume remains occupied by unhydrated cement); if the w/c is high, then complete hydration may occur ($X=1$) while capillary pores persist.

The BNG model does not take account of the change in volume of the body during the reaction. It is not the chemical shrinkage that matters, because that does not change the dimensions of the body (because the sample in a chemical shrinkage experiment is small, and is surrounded by excess water). It is autogenous shrinkage, caused by capillary pressure as air enters the pores (after setting), that changes the volume of the body. To take this into account, it would be necessary to correct the denominator in Eq. (8) by a factor of $1+\varepsilon_A$, where ε_A (<0) is the volumetric autogenous shrinkage. The autogenous shrinkage cannot be calculated from the chemical shrinkage, so a separate measurement would be required to correct for it; fortunately, ε_A is small, so the correction can generally be ignored. That is, X provides a good measure of the actual volume fraction occupied by hydration products, and it is proportional to the chemical shrinkage and the degree of hydration.

2.2. BNG model — constant nucleation rate

Cahn [15] extended the JMAK model to describe the case where nucleation occurs on grain boundaries, as in recrystallization of metals, rather than occurring randomly throughout the volume. That situation bears some similarity to the case of hydration of cement, where the reaction product forms directly on the surface of the cement grains [21], but there are some significant differences. Firstly, a crystal of metal that nucleates on a grain boundary will grow at equal rates on both sides of the boundary, as indicated in Fig. 2a. In contrast, if a hydration product nucleates on the surface of a clinker grain, it will grow at different rates into the grain and into the water-filled interstitial space, as in Fig. 2b or c. Secondly, the growth rate might be anisotropic. It has been observed that the primary particles of C-S-H are nonspherical [17,22], but that does not mean that the hydrate (which is an assemblage of such particles) will grow anisotropically, since the primary particles are not necessarily aligned. Nevertheless, it is possible to allow for ellipsoidal growth, so the general case is presented. Thirdly, more than one phase may be hydrating simultaneously. We will deal with that complication in Section 2.4. Finally, the process of impingement of hydration products is not the same as envisaged in Cahn's model, where the growth of the product on a given boundary can be interrupted by collision with a particle growing from a nucleation site that is arbitrarily distant. During hydration, the product growing from the surface of a particle of clinker cannot grow through the surface of an adjacent clinker particle, so its growth is confined in the pore space, and it can be blocked either by the bare surface of an opposing grain, or the product growing on that surface. If the nucleation rate is low, then impingement of the hydration product is most likely to be blocked by the bare surfaces of adjacent clinker grains, which violates the assumption of Cahn's model (*viz.*, that the nucleating surface cannot block growth). On the other hand, if the nucleation rate is high enough, then the surface of every grain will be covered with product before a particle nucleated on an adjacent grain can grow into contact. In that case, impingement is dominated by the product growing on neighboring particles, so the inability of distant nuclei to block growth is irrelevant. Therefore, we expect the present model to be satisfactory when the fraction of surface area covered with product is near unity at the setting point, when contacts between particles percolate.

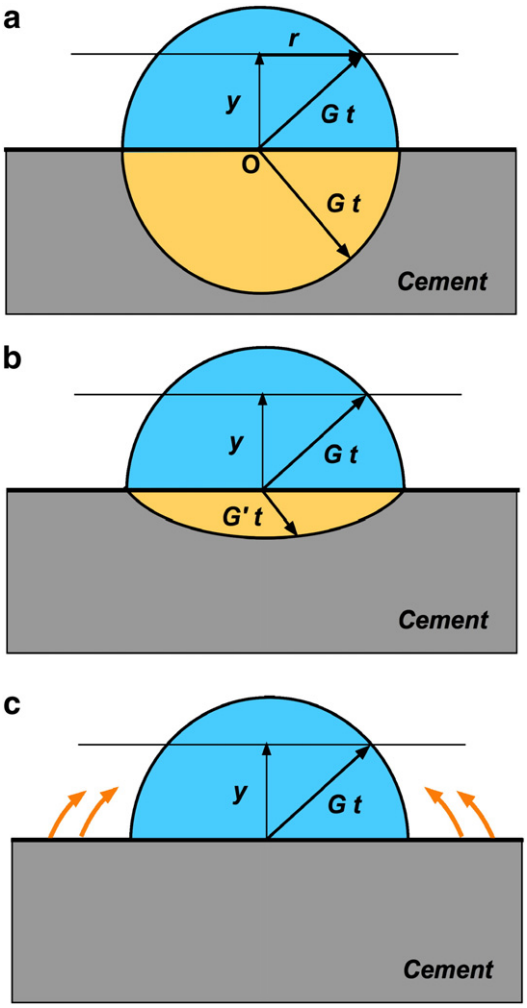

Fig. 2. Schematic illustration of particle nucleated on the surface of a cement grain. (a) Growth occurs at the same rate, G, in both directions (*i.e.*, into the cement grain, which is shaded gray, and into the water-filled surrounding space); (b) the growth rate into the grain, G', is different from that into the surrounding space, G; (c) no growth occurs into the grain ($G'\approx 0$). The arrows in (c) imply that the reactants travel to the particle from the exposed surface of the grain, with negligible transport through the particle. In (a) or (b), some transport through the particle would be necessary.

In the following, we closely follow Cahn's procedure, but allow for the growth rate to be different in each of the orthogonal directions. As shown in Fig. 3, an ellipsoidal particle results from a nucleation event at time τ, followed by growth at rates G_1, G_2, and G_3 along the x, y, and z directions. The growth rates are assumed to be constant in time, although this is not strictly justifiable; the time dependence of the supersaturation, and its impact on the kinetics of hydration, are presently under study [23]. In the following, the word "particle" refers to the hydrate that grows from a single nucleus; the internal structure (size and packing of primary particles) is not considered further. We assume that the substrate (*i.e.*, the surface of the cement

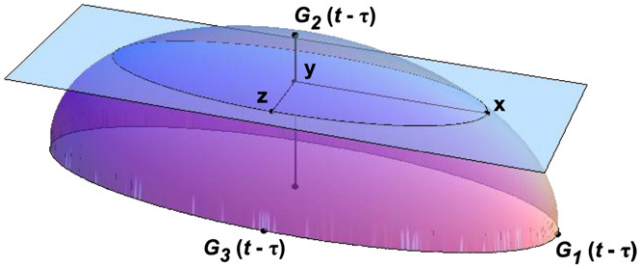

Fig. 3. Schematic of elliptical particle with axis dimensions $x_{max}=G_1(t-\tau)$, $y_{max}=G_2(t-\tau)$, and $z_{max}=G_3(t-\tau)$. A plane at height y intersects the particle in an ellipse with major axis x and minor axis z.

grain) is flat. Bishnoi and Scrivener [24] attempted to correct for the curvature of a spherical substrate, but that is an unnecessary complication, as long as the nucleation rate is high. That is, if the particles are close enough so that they impinge laterally while they are still much smaller than the diameter of the grain, then the curvature effect is negligible. The surface of the ellipsoid in Fig. 3 is described by

$$\left(\frac{x}{G_1(t-\tau)}\right)^2+\left(\frac{y}{G_2(t-\tau)}\right)^2+\left(\frac{z}{G_3(t-\tau)}\right)^2=1. \tag{11}$$

A plane at height y above the substrate intersects the particle in an ellipse whose semi-major and semi-minor axes are

$$x=G_1(t-\tau)\sqrt{1-\left(\frac{y}{G_2(t-\tau)}\right)^2},\ y\le G_2(t-\tau) \tag{12}$$

and

$$z=G_3(t-\tau)\sqrt{1-\left(\frac{y}{G_2(t-\tau)}\right)^2},\ y\le G_2(t-\tau). \tag{13}$$

The area of the elliptical intersection is

$$A_E(y)=\pi xz=\begin{cases}\pi g\left(G_2^2(t-\tau)^2-y^2\right), & y\le G_2(t-\tau)\\ 0, & y>G_2(t-\tau)\end{cases} \tag{14}$$

where g is a parameter indicating the degree of anisotropy of the growth rate,

$$g=\frac{G_1G_3}{G_2^2}. \tag{15}$$

In Cahn's model, the growth is isotropic, so $g=1$; for the prolate ellipsoids considered by Bishnoi and Scrivener [24] and Garrault and Nonat [25], $G_1=G_3$ so $g=(G_1/G_2)^2$. The volume of the particle between the substrate and the plane at y is

$$V(y)=\int_0^y A_E\left(y'\right)dy'=\frac{\pi}{3}gy\left(3G_2^2(t-\tau)^2-y^2\right),\ G_2(t-\tau)>y. \tag{16}$$

If the nucleation rate is constant at I_B (events per unit area of substrate per unit time), then the extended area fraction (*i.e.*, neglecting overlap) from particles nucleated between time τ and $\tau+d\tau$ is

$$dY_e=A_E(y)I_Bd\tau,\ G_2(t-\tau)>y \tag{17}$$

so

$$Y_e=\int_0^t A_E(y)I_Bd\tau=\frac{\pi}{3}gG_2^2I_Bt^3(1-u)^2(1+2u),\ u<1 \tag{18}$$

where $u=y/(G_2t)$. The actual area fraction (allowing for overlap from nucleation sites that are randomly located on the substrate) is

$$Y(y,t)=1-\exp(-Y_e). \tag{19}$$

The use of Eq. (19) to correct for impingement is valid only if the axes of the elliptical particles are randomly oriented and blocking does not occur. Consider a point, P, on the surface of a grain that is near a growing particle; if another particle is nearby with its fast growth direction oriented across the path from P to the first particle, then the second particle may grow across the path and block the first particle from growing over (and thus transforming) point P. When the particle growth rates are highly anisotropic, this type of blocking reduces the probability of transformation of any point on the surface. Birnie and Weinberg [26] examined this problem for two-dimensional cases. Unfortunately, correcting for this phenomenon is very complicated, so we must recognize that the present analysis is valid only for modest degrees of anisotropy. For example, in the 2-D case, when the anisotropy (G_2/G_1) is<5, the error from blocking only becomes significant when more than ~2/3 of the area is transformed.

The volume of particles originating from a unit area of the substrate is

$$\begin{aligned}V_0&=2r_G\int_0^\infty Ydy\\&=2r_GG_2t\int_0^1\left(1-\exp\left[-\frac{\pi}{3}gG_2^2I_Bt^3(1-u)^2(1+2u)\right]\right)du\end{aligned} \tag{20}$$

where we introduce the factor r_G, which is the ratio of the growth rates into and out of the substrate. If the growth is symmetrical, as assumed by Cahn [15] and Thomas [9] (see Fig. 2a), then $r_G=1$; if the particle does not grow into the substrate, as in Fig. 2c, then $r_G=1/2$. At the beginning of the process, when most of the grain is exposed to water, it is likely that $r_G\approx1/2$, because all of the species feeding growth of the particle are delivered from the adjacent bare surface, with little contribution from species moving through the particle from the underlying grain. As the grain becomes covered with hydration products, the situation is likely to resemble Fig. 2b (with outer product growing into the pore liquid and inner product growing into the grain), so that r_G lies between 1/2 and 1. The use of this factor lacks rigor, because Cahn's model requires that the growth from any given nucleation site can be blocked by growth from a distant site, but that is not true for the hydration products. The growth of the product inside a grain can never be blocked by outer product nucleated on an adjacent (or more distant) particle. Therefore, we can only expect the use of r_G to be valid when the nucleation rate is so high that the outer product impinges on product on adjacent grains, and the inner product forms a layer inside the clinker grain, so that it impinges only on inner product in its own grain. If the nucleation rate were low, then the equation would not exclude the unphysical situation in which inner product from one grain penetrates a neighboring grain. The growth of the inner product is better described by models in which growth is not permitted to cross the boundaries of the particle. Theories of that kind have been developed by several authors [12,27,28], and will be discussed elsewhere [29] as models for hydration. It is shown in Ref. [29] that excellent fits can be obtained with models based on distinctly different assumptions, indicating that one cannot infer the operative mechanisms on the basis of the quality of the fit to BNG models.

The extended volume fraction of hydration products from a boundary area O_v^B of cement per unit volume of paste is

$$X_e=O_v^BV_0=2O_v^Br_GG_2t\int_0^1 Ydu. \tag{21}$$

The area of substrate per unit volume of paste is related to the specific surface area of the cement, S (area per mass of cement) by

$$O_v^B = \frac{S}{R_{wc}/\rho_w + 1/\rho_c}. \tag{22}$$

To see the physical significance of this quantity, suppose that a spherical envelope of water is applied to each particle with a thickness such that the w/c within the envelope is R_{wc}. If the radius of the envelope is r_E, then $O_v^B = 3/r_E$, so r_E is effectively the size of the "reaction vessel" in which hydration occurs. The total volume fraction of hydration products is

$$X = 1 - \exp(-X_e). \tag{23}$$

Eq. (23) is valid if the grain surfaces are randomly oriented and growth blocking is not significant. The latter condition can be satisfied if the growth anisotropy is modest, but the acceptable degree of anisotropy is difficult to quantify. If the hydration products are anisotropic, but aligned normal to the grain, then blocking is less probable, and Eq. (23) should provide a good approximation.

Defining the following constants,

$$k_B = \left(g r_G I_B O_v^B\right)^{1/4} G_2^{3/4} \tag{24}$$

$$k_G = r_G O_v^B G_2 \tag{25}$$

$$k_Y = \frac{\pi}{3}\frac{k_B^4}{k_G} = \frac{\pi}{3} g G_2^2 I_B \tag{26}$$

we can write Eq. (21) as

$$X_e = 2k_G t \int_0^1 \left(1 - \exp\left[-k_Y t^3 (1-u)^2 (1+2u)\right]\right) du. \tag{27}$$

Both k_B and k_G have units of reciprocal time: $1/k_G$ is the time for the hydration product to grow a distance roughly equal to the radius of the "reaction vessel", r_E, and $1/k_B$ is roughly the time for the extended volume fraction to reach unity. The constant k_Y has units of reciprocal time cubed, and we see from Eq. (18) that $1/k_Y^{1/3}$ is the time required for the extended area fraction of product on the surface of the cement to reach unity.

The actual volume fraction of products is obtained by using Eq. (27) in Eq. (23):

$$X(t) = 1 - \exp\left[-2k_G t \int_0^1 \left(1 - \exp\left[-k_Y t^3 (1-u)^2 (1+2u)\right]\right) du\right]. \tag{28}$$

At long times, this reduces to

$$X \approx 1 - \exp(-2k_G t), k_Y t^3 \gg 1. \tag{29}$$

This equation describes the growth of a uniform layer of product normal to the substrate at a rate G_2, after lateral growth of the individual particles causes them to coalesce into a layer.

The growth anisotropy ratio, g, only appears in a product with the nucleation rate, I_B. When g or I_B is large, the product layer spreads laterally over the surface and coalesces into a uniform layer while it is still relatively thin. Conversely, if g is small, it means that the growth rate outward from the surface is fast compared to its lateral spreading rate; in this case, or if nucleation is sparse (*i.e.*, I_B is small), then the product layer extends far from the grain before the particles impinge on one another. In the latter case, the present solution will overestimate the rate of transformation, owing to neglect of growth blocking. Garrault and Nonat [19,25] concluded that G_2/G_1 is about 3–6, which would be near the level at which growth blocking might complicate the calculation [26].

The fraction of the surface of the grain that is covered with product is found by setting $u = 0$ in Eq. (18) and using Eq. (19). The result is

$$Y(0,t) = 1 - \exp\left(-k_Y t^3\right). \tag{30}$$

When growth is isotropic ($g = 1$) and bidirectional ($r_G = 1$), the preceding results are identical to those obtained by Cahn [15] and used by Thomas [9] to describe calorimetric data for hydration of C_3S. The constant k_G defined in Eq. (25) differs by a factor of r_G from the constant used in Ref. [16].

When $X \ll 1$, expansion of Eq. (28) leads to

$$X \approx X_e \approx \frac{\pi}{3}(k_B t)^4 \approx \frac{\pi}{3} r_G \left(I_B O_v^B\right)(G_1 G_2 G_3) t^4. \tag{31}$$

The quality of the approximation, shown in Fig. 4, depends strongly on the ratio of k_B to k_G. When that ratio is large, it means that the nucleation rate is high, so there are many particles growing that impinge on one another when X is small, so the approximation fails early; when the ratio is small, there are widely separated particles that can produce a substantial degree of transformation before they impinge, so the approximation is useful for larger X.

2.3. BNG model — constant number of nuclei

If nuclei are created by a rapid burst of nucleation at time τ, or are initially present ($\tau = 0$), the preceding analysis is simplified. This situation is often called "site saturation". If the number of nuclei per unit area of the grain surface has the constant value N_S, then Eq. (18) is replaced by

$$Y_e = N_S A(y) = \pi N_S g G_2^2 (t-\tau)^2 \left(1 - u^2\right), \; u < 1 \tag{32}$$

where $u = y/[G_2(t-\tau)]$. If N_S nuclei are initially present and new nuclei continue to form on the exposed boundary at a constant rate, then Eqs. (18) and (32) can be added together. Cahn [15] provided that solution, for isotropic growth, as his Eq. (12).

Eqs. (19) and (21) still apply, but Eq. (27) is replaced by

$$X_e = 2k_G(t-\tau) \int_0^1 \left(1 - \exp\left[-k_S^2 (t-\tau)^2 \left(1 - u^2\right)\right]\right) du \tag{33}$$

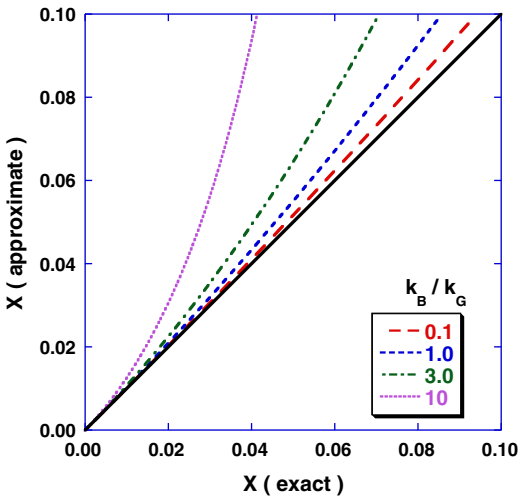

Fig. 4. Comparison of approximation from Eq. (31) with exact result from Eqs. (23) and (27) for various values of the ratio k_B/k_G.

where

$$k_S = \sqrt{\pi N_S g} G_2. \tag{34}$$

From Eq. (32), we see that $1/k_S$ is the time at which the extended area of reaction product on the surface of the cement reaches unity.

As in the previous case, the growth anisotropy factor and the nucleation density only occur in a product. The fraction of the surface of the grain that is covered with hydration products is found by setting $u=0$ in Eq. (32) and substituting into Eq. (19). The result is

$$Y(0,t) = 1 - \exp\left[-k_S^2 (t-\tau)^2\right] \tag{35}$$

so coverage is 95% complete when $t \approx 1.7/k_S$. As explained earlier, this result is valid only if the anisotropy is modest. The integral in Eq. (33) can be evaluated in terms of the Dawson F-function, defined by

$$F_D(x) = \exp\left(-x^2\right) \int_0^x \exp\left(y^2\right) dy. \tag{36}$$

The result is

$$X_e = 2k_G(t-\tau)\left(1 - \frac{F_D[k_S(t-\tau)]}{k_S(t-\tau)}\right) \tag{37}$$

so, if the anisotropy is not too great,

$$X(t) = 1 - \exp\left[-2k_G(t-\tau)\left(1 - \frac{F_D[k_S(t-\tau)]}{k_S(t-\tau)}\right)\right]. \tag{38}$$

When $X \ll 1$, the expansion of Eq. (38) is

$$X(t) \approx \frac{4}{3} k_G k_S^2 (t-\tau)^3 \approx \frac{4\pi}{3} r_G \left(N_S O_v^B\right)(G_1 G_2 G_3)(t-\tau)^3. \tag{39}$$

This approximation is compared to the exact result, Eq. (38), in Fig. 5. When $k_S(t-\tau) \gg 1$, then Eq. (38) approaches

$$X(t) \approx 1 - \exp[-2k_G(t-\tau)], k_S(t-\tau) \gg 1 \tag{40}$$

which is equivalent to the result given by Cahn [15] for the case where nucleation sites become saturated at long times. This equation describes the growth of a uniform layer of product normal to the substrate at a rate G_2; that is, the individual particles spreading from the N_S nuclei per unit area have coalesced into a layer.

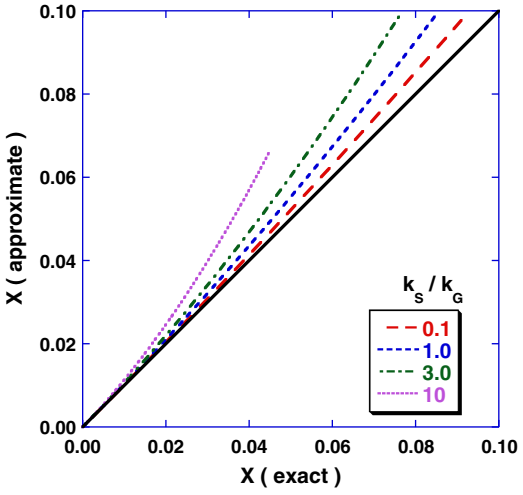

Fig. 5. Comparison of approximation from Eq. (39) with exact result from Eq. (38) for various values of the ratio k_B/k_G.

2.4. Multiple phases

The preceding analysis is intended to describe the transformation of one phase into another; however, ordinary Portland cement contains four phases capable of hydration (C_3A, C_3S, C_2S, C_4AF), so the amount of product is a weighted average of the volume fraction of each that has reacted. If the reaction rates were widely different, so that only one phase was reacting at a time, then the kinetics at any given time would be the sum of a constant (representing the inert phases) plus Eq. (28) (representing the single reacting phase). Unfortunately, the situation is not so simple for cement, so it should not be expected that a single function, such as Eq. (38) for example, would describe the complete hydration process. If the focus is on the period around initial setting, then such an analysis should be quite useful, because the initial reaction of the aluminates is done in a few minutes (so it can be treated as constant) and the slower-reacting phases (*viz.*, C_2S and C_4AF) are not making a substantial contribution yet. As long as the setting process is dominated by the hydration of C_3S, the nucleation and growth models should provide a good description, and experience indicates that they do. In this case, the equation fitted to the data should have the form

$$\frac{F(t)}{F(\infty)} = f_{C3A} + f_{C3S} X_{C3S}(t) \tag{41}$$

where F is the property being measured (such as heat released or chemical shrinkage) and f_k is the fraction of that property contributed by phase k when the hydration is complete. This is the form generally used in the literature.

The difficulty for the experimentalist is to know the time beyond which the model is no longer valid. For example, once the degree of hydration of C_2S becomes significant, then the contribution of X_{C2S} must be incorporated into Eq. (41); the effects are not simply additive, because the growth of a given phase is not only blocked by that phase, but by all the phases that are forming [30]. As a practical matter, this introduces so many constants into the fitting that none of them can be reliably fixed. A serious additional problem is that the models assume that the growth rates of the phases are constant, which is apparently valid during the early part of the hydration, because the supersaturation is approximately constant [10,11], but which ceases to be valid if the growth becomes controlled by the rate of diffusion of ions. Indeed, work by Nonat's group suggests that diffusion control is established as soon as the surface of the grain is covered with reaction products [19,25,31]. By the time that the hydration of C_2S must be taken into account, the rate of reaction of C_3S may be diffusion controlled. Moreover, owing to the coverage of the cement grain with hydration products, the reaction of C_2S might be diffusion controlled from the outset. On the other hand, it has been argued by Thomas [32] that the transition to diffusion control must occur long after the peak, because there is no change in activation energy before that. Given these complications, it is probably not justifiable to apply a BNG analysis to hydration data much beyond the final setting time.

3. Comparison to chemical shrinkage data

Measurements of the chemical shrinkage of Class H cement were presented in Ref. [16] and analyzed using the BNG model in the form used by Thomas [9]. In the following, we fit the same data to the model from Section 2.3, where the number of nuclei is fixed. This is more consistent with the predictions of simulations by Bullard [10], which show that the supersaturation is high enough to cause nucleation only during the first few minutes of hydration of C_3S. In reality, there should be a time-varying rate of nucleation during a short period, but we will assume that it is over before we begin our measurements, which start about 20 min after contact between the

cement and water. Moreover, we assume that the period during which nucleation occurs is negligible compared to the duration of the experiment, so we let $\tau = 0$ (although it could be left as a free parameter). Thus, we fit the chemical shrinkage data to

$$s(t) = s_0 + A\left\{1 - \exp\left[-2k_G t\left(1 - \frac{F_D[k_S t]}{k_S t}\right)\right]\right\} \tag{42}$$

where s_0 is a baseline adjustment to take account of the early reactions that are not detected and A the constant of proportionality between shrinkage and degree of reaction; in principle, it should equal the constant from Eq. (10) times the volume fraction of C_3S in the cement. Thus, there are 4 free constants for the fit: s_0, A, k_G, and k_S.

To fit data from calorimetric experiments, which directly report the *rate* of heat release, we need to use the time derivative of Eq. (42):

$$\frac{ds}{dt} = 4Ak_G k_S t F_D[k_S t] \exp\left[-2k_G t\left(1 - \frac{F_D[k_S t]}{k_S t}\right)\right]. \tag{43}$$

In Section 4, we will use simultaneous fits to Eqs. (42) and (43) to find the four parameters.

3.1. Fits with constant nucleation rate

Before considering the new fits, we must re-interpret the constants from the fits based on the model assuming a constant rate of nucleation. One of the principle conclusions of the experimental study [16] was that the degree of hydration at the initial setting point, α_{set}, was independent of temperature or the presence of chemical additives: $\alpha_{set} = 0.0388 \pm 0.0038$ when w/c = 0.35. According to Eq. (9), X is proportional to α, so we can approximate the relationship between α_{set} and t_{set} using Eq. (31):

$$\frac{\alpha_{set}}{B} \approx X_{set} \approx \frac{\pi}{3}(k_B t_{set})^4. \tag{44}$$

This implies a hyperbolic relationship between t_{set} and k_B,

$$t_{set} \approx \left(\frac{3\alpha_{set}}{\pi B}\right)^{1/4} \Big/ k_B. \tag{45}$$

A relationship of this kind was demonstrated in Ref. [16], but the constant of proportionality was 0.62, whereas Eq. (45) predicts ~0.43.

A more accurate result is obtained from Eq. (28), which can be written as

$$\frac{\alpha}{B} = 1 - \exp\left[-\frac{2\theta}{k}\int_0^1 \left(1 - \exp\left[-\frac{\pi}{3}k\theta^3(1-u)^2(1+2u)\right]\right)du\right] \tag{46}$$

where $\theta = k_B\, t$ and $k = k_B/k_G$. When θ is small, the factors of k cancel out, and Eq. (46) reduces to Eq. (44), but for longer times the more complicated form is required. In terms of the constants defined in the present paper, for Class H cement at w/c = 0.35, the fits to the chemical shrinkage data indicate that $k \approx 2$–3. For that value, along with $\alpha_{set} \approx 0.039$ and $B \approx 1.1$, we find from Eq. (46) that $\theta = k_B t_{set} \approx 0.53$, which is in fair agreement with the experimental value of 0.62. The existence of this relationship between k_B and t_{set} simply confirms that the setting point corresponds to a fixed degree of hydration. The discrepancy in the value of the constant of proportionality may be associated with the low density of the initial product, which is discussed in Section 5.

The fraction of the surface of the cement grains that is covered with hydration products at the time of initial setting, Y_{set}, can be estimated from Eq. (30):

$$Y_{set} \equiv Y(0, t_{set}) = 1 - \exp\left(-k_Y t_{set}^3\right). \tag{47}$$

For Class H cement, Y_{set} is found to be about 0.62 ± 0.05 for 9 experiments at w/c = 0.35 at temperatures from 10 to 60 °C. As explained earlier, this means that the use of Cahn's model is reasonable, because the surface coverage is so high that impingement generally occurs on hydration product from the adjacent grain.

3.2. Fits with constant number of nuclei

When the chemical shrinkage data from Ref. [16] are fit to Eq. (42), the fits to the shrinkage curves are very similar to those obtained by assuming that I_B is constant; however, the derivative curves are fit slightly better by the model with constant N_S. Typical results are shown in Fig. 6 for Class H cement at w/c = 0.35 and $T = 25$ °C. For this sample, the initial setting time from the Vicat needle test is 5.5 h and the data extend to 95 h. If the fits are done over different time intervals (12, 24, 48, 72, 95 h), the standard deviation of the fitting parameters is <10% of the mean. The fits over the first 24–48 h are most meaningful, because a reproducible inflection occurs after ~40 h at 25 °C, as shown in Fig. 8. This apparently reflects the hydration of a different phase in the cement,

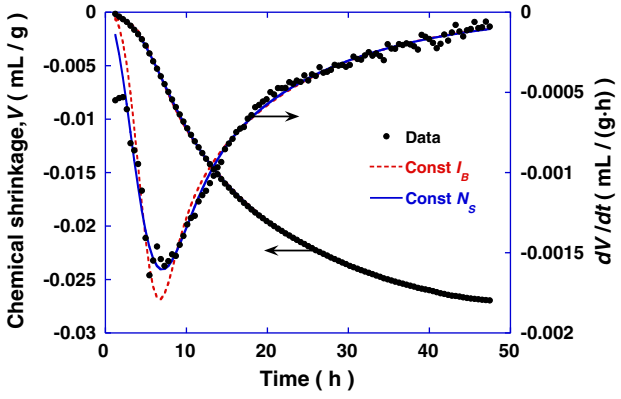

Fig. 6. Comparison of fits to chemical shrinkage data (left axis) for Class H cement (w/c = 0.35, $T = 25$ °C) from Ref. [16]. The slope of the shrinkage (right axis) is slightly more accurately fit by the model assuming a constant number of nuclei (Const N_S) than the model assuming a constant nucleation rate (Const I_B).

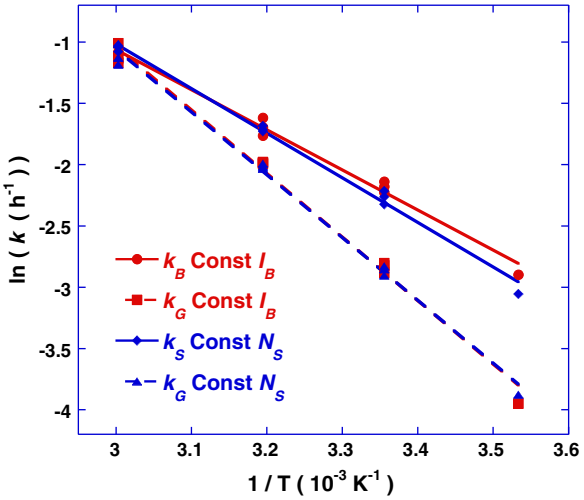

Fig. 7. Temperature dependence of fitting parameters for models assuming constant nucleation rate (Const I_B) or constant number of nuclei (Const N_S). Fits were applied to chemical shrinkage data for Class H cement with w/c = 0.35 from Ref. [16].

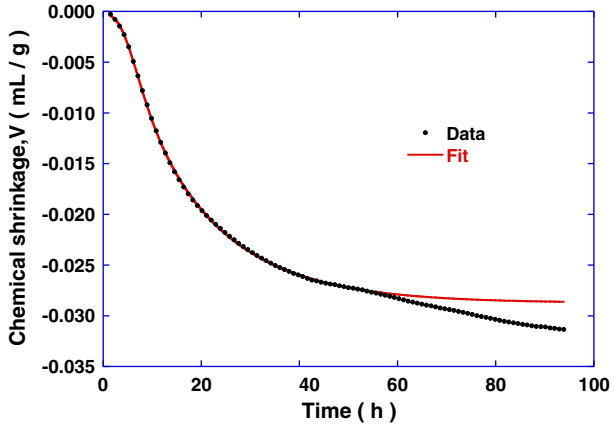

Fig. 8. Chemical shrinkage data for Class H cement (w/c = 0.35, 25 °C) with curve calculated from Eq. (42) with parameters obtained by fitting data up to 48 h. The inflection near 50 h is attributed to the onset of hydration of another component of the cement or to a change in the density of the product (*e.g.*, in-filling of the C-S-H).

so another $X(t)$ function would have to be added to describe the later part of the experiment. The temperature dependence of the fitting parameters (obtained for data preceding the inflection) is shown in Fig. 7. The results for the two models are essentially identical. The activation energy is 42.6 kJ/mol for k_G and 30.2 kJ/mol for k_S.

From Eqs. (25) and (34), we find that the number of nuclei per unit area of the cement particle is

$$N_S = \frac{\left(O_v^B r_G\right)^2}{\pi g}\left(\frac{k_S}{k_G}\right)^2. \tag{48}$$

For the cement used in these experiments, the surface area measured by the BET method was 1.0 m^2/g, so Eq. (22) indicates that $O_v^B = 1.50\times10^6\ m^{-1} = 1.50\ \mu m^{-1}$. Assuming that $g=1$ and $r_G=1$, the number of nuclei per μm^2 is shown in Fig. 9. At 25 °C, $N_S \approx 6\ \mu m^{-2}$, which is the same order of magnitude (~1.4/μm^2) as was found [33] for nucleation on C_3S in simulations done with HydratiCA [10]. Assuming that $r_G=0.5$ would reduce our estimate of N_S to 1.5 μm^{-2}; however, if g is as small as indicated by the simulations done by Garrault and Nonat [25], then N_S is an order of magnitude larger. Fig. 9 shows that N_S decreases as temperature

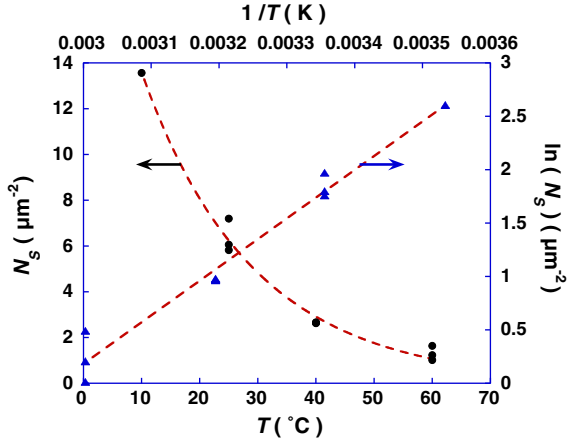

Fig. 9. Number of nuclei per square micron, N_S, calculated from fits to chemical shrinkage of Class H cement (w/c = 0.35, BET area = 1.0 m^2/g), assuming isotropic growth ($g=1$) and no penetration of hydration products into the grain ($r_G=1$). Left ordinate and lower abscissa: N_S *versus* T (°C); Right ordinate and upper abscissa: ln(N_S) *versus* $1/T$ (K).

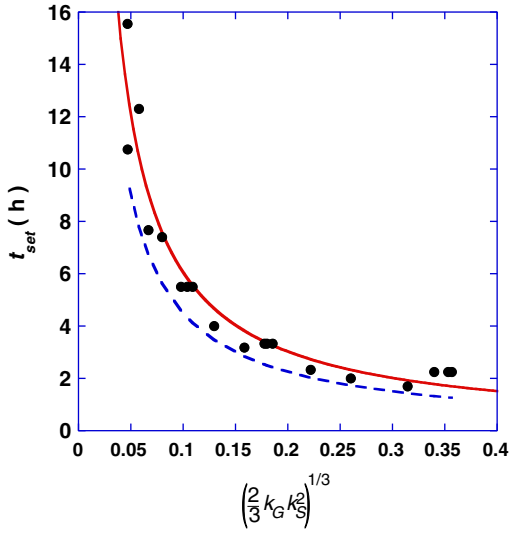

Fig. 10. Solid curve is a fit of Eq. (49) to measured setting time for Class H cement for w/c ratios of 0.25, 0.35, and 0.40 at temperatures of 10–60 °C, with and without chemical additives; setting time data from Ref. [16]. Dashed curve is obtained from Eq. (50).

increases, which implies that the supersaturation is lower at elevated temperatures.

According to Eq. (35), coverage of the cement grains with hydration products is 95% complete when $t \approx 1.7/k_S$. From the fits to Class H cement, this time is about 16–17 h at 25 °C, but rises to 36 h at 10 °C, and drops to 9.5 and 5 h at 40 and 60 °C, respectively.

The relationship between the degree of hydration and the setting time for this model that is equivalent to Eq. (44) is found from Eq. (39):

$$t_{set} \approx \tau + \left(\frac{\alpha_{set}}{B}\right)^{1/3} \Big/ \left(\frac{4}{3}k_G k_S^2\right)^{1/3}. \tag{49}$$

As shown in Fig. 10, this relationship fits the data for Class H cement very well with $\tau=0$, but the constant of proportionality is 0.61, whereas $(\alpha_{set}/B)^{1/3} \approx 0.33$. Better agreement is obtained by using Eq. (38):

$$\frac{\alpha}{B} = 1 - \exp\left[-\left(\frac{2k_G}{k_S}\right)(\theta - F_D[\theta])\right] \tag{50}$$

where $\theta = k_S(t-\tau)$. For the Class H cement, $k_G/k_S \approx 1.6 \pm 0.4$; in that range, with $\alpha = \alpha_{set} = 0.039$ and $B \approx 1.1$, Eq. (50) yields $\theta = 0.41$ to 0.49. Thus, $t_{set} \approx 0.45/k_S \approx 0.46/(2k_G k_S^2/3)^{1/3}$; the dashed curve in Fig. 10 shows this relationship.

A set of experiments was done on the same cement with the addition of various amounts of $CaCl_2$ to accelerate the hydration [16]. Fig. 11 shows the results of simultaneously fitting Eqs. (42) and (43) to those data, assuming constant N_S. For the highest concentration of $CaCl_2$ the fit does not quite capture the sharp peak of the shrinkage rate curve. Using a constant rate of nucleation, rather than a constant number of nuclei, very slightly improves the fit to the peak, but correspondingly degrades the fit to the shrinkage curve, especially at longer times; further improvement might be obtained by allowing some initial sites in addition to a constant nucleation rate, but that was not tested. As shown in Fig. 12, the fitting parameters vary smoothly with the concentration of accelerator. Since k_S and k_G are both proportional to the growth rate, and both rise by a factor of 3, we conclude that the 2% chloride additions enhance the growth rate by that amount, and the nucleation density, N_S, changes by <20%.

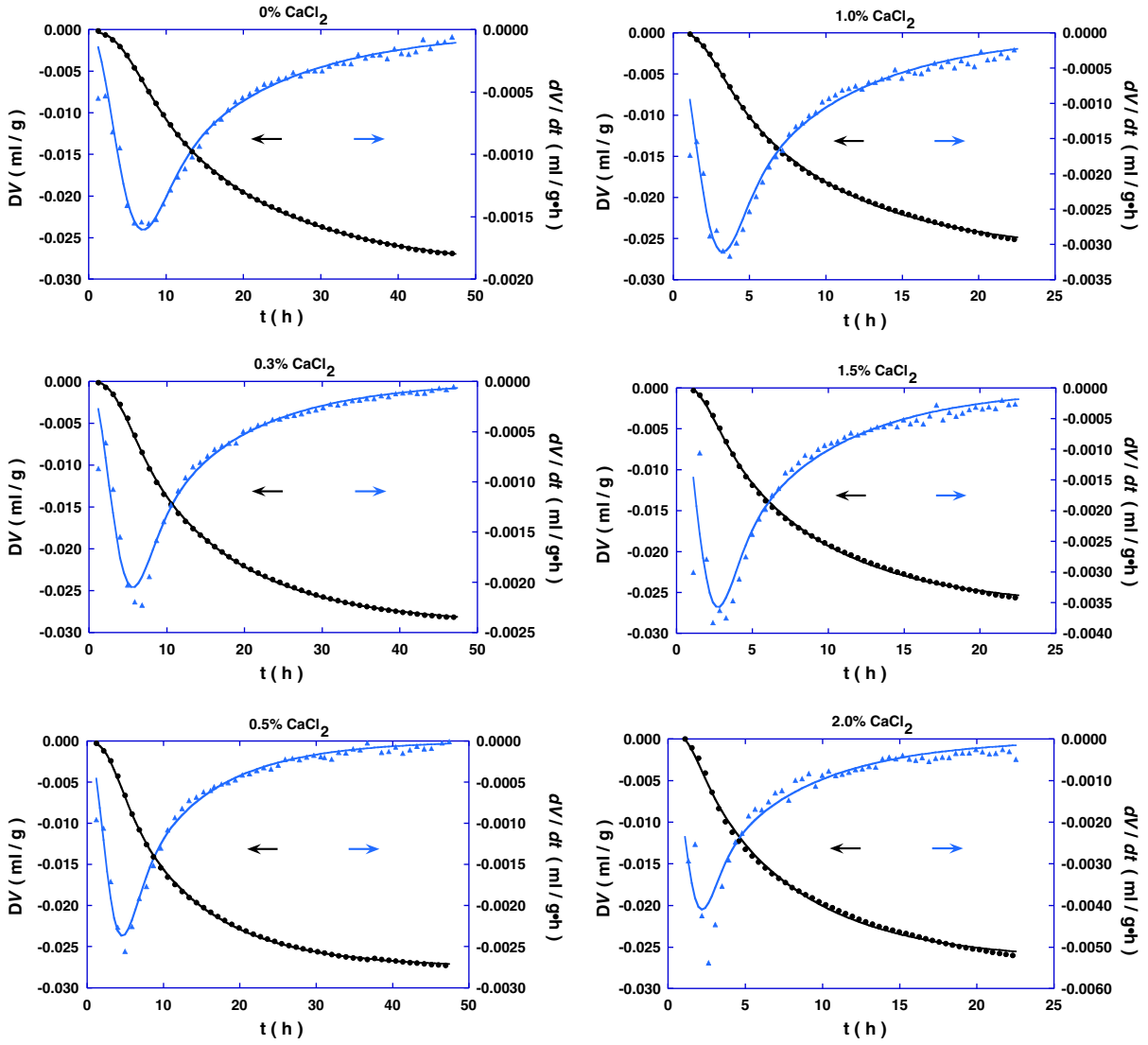

Fig. 11. Chemical shrinkage data from Ref. [16] for Class H cement at 25 °C, w/c = 0.35, with $CaCl_2$ additions of 0, 0.3, 0.5, 1.0, 1.5, and 2.0 wt.%. Curves are from simultaneous fits to Eqs. (42) and (43), assuming growth from a constant number of nuclei.

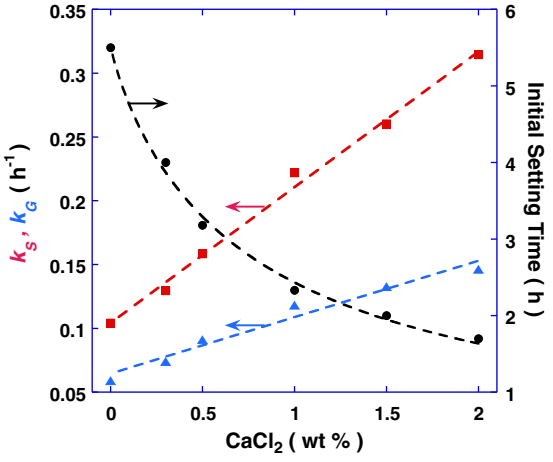

Fig. 12. Parameters obtained from the fits shown in Fig. 11 (left ordinate) and initial setting time from the Vicat test for those samples [16], showing the trend with concentration of $CaCl_2$.

4. Comparison to calorimetric data

Bishnoi and Scrivener [24] performed a series of calorimetric measurements on the hydration of alite on powders with narrow particle size distributions. Fits to these data should yield similar values of growth rate and nucleation density (allowing for variations in mineralogy and defect concentration in particles of different sizes), since the size fractions were separated from the same source. In Fig. 13, we show the results of simultaneously fitting Eqs. (42) and (43) to those data over the time interval from 3 to 24 h. As indicated in Table 3, $k_S = 0.061 \pm 0.016\ h^{-1}$ for the five sets of data; since this parameter, defined in Eq. (34), involves both the nucleation density and growth rate, we conclude that the fits are internally consistent. To separate the growth rate, G_2, and density of nuclei, N_S, it is necessary to know the relative growth rates of inner and outer product, r_G, the growth anisotropy, g, and the surface area per unit volume, O_v^B. Assuming that $r_G = g = 1$ and using the BET surface area (reported for sets A–D) and w/c = 0.4 to calculate O_v^B, we find $G_2 = 0.084 \pm 0.029\ \mu m/h$; a wider range is found for N_S ($0.24 \pm 0.26\ \mu m^{-2}$), but it is more sensitive to the unknown parameters.

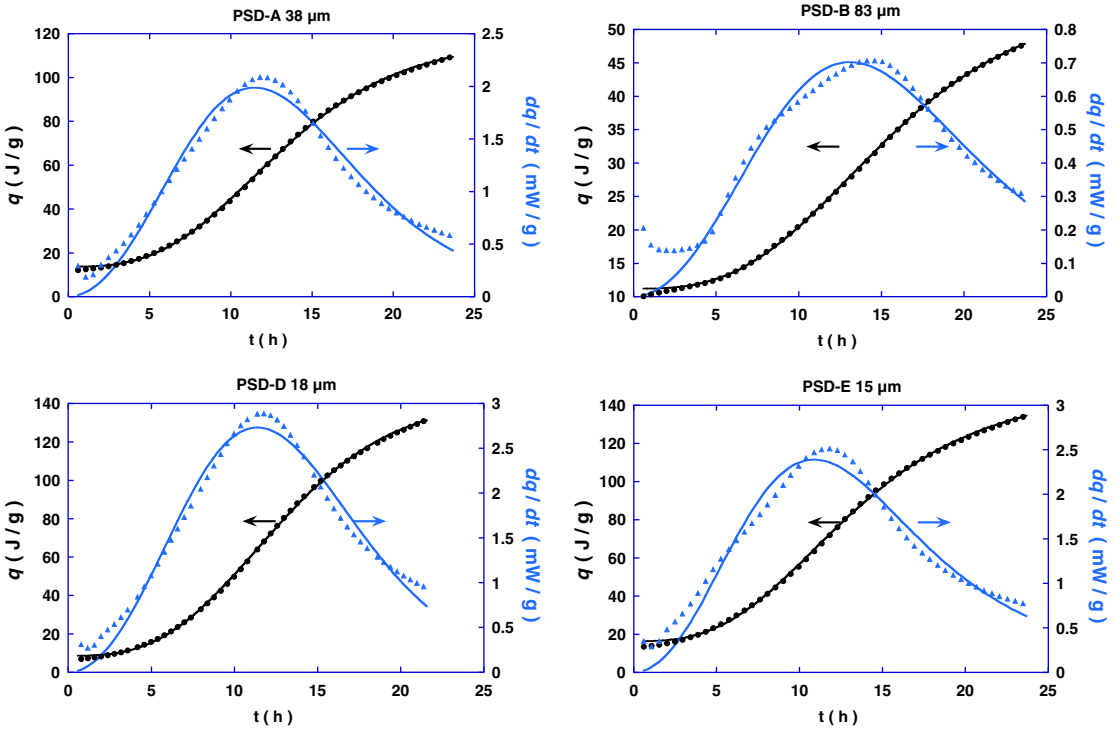

Fig. 13. Simultaneous fits of Eqs. (42) and (43) to calorimetric data from Ref. [24] for hydration of alite, assuming growth from a constant number of nuclei. PSD-A is unfractionated alite with a modal particle diameter of 38 μm; the other samples are narrow distributions with the indicated modal value.

5. Discussion

The most striking thing about the fits using the two models is that they are so similar, as illustrated by Fig. 6. Assuming that growth occurs from a constant number of nuclei results in slightly better fits at temperatures from 10 to 40 °C; assuming a constant nucleation rate yields slightly better results at 60 °C, but the data are noisier at that temperature. The temperature dependences of the constants are identical, as demonstrated by Fig. 7. This means that it is impractical to determine the mechanism of the transformation from the quality of the fit. However, sophisticated simulations of the reaction [10] indicate that nucleation occurs in a short burst, so the model based on a constant number of nuclei has independent support. The nucleation frequency shown in Fig. 9 is also similar to that found from the simulation [33]. Since the area per nucleus is found to be about 0.1 μm^2, the particles will not be sensitive to the curvature of the particle; that is, with such a high nucleation frequency, it is not necessary to take account of the curvature of the grain. In any case, since real cement particles are irregular in shape, corrections that assume a spherical shape for the grain [*e.g.*, 24] would not necessarily improve the accuracy of the calculation.

Fig. 14 shows that k_G is nearly independent of the water/cement ratio, but k_S increases as w/c decreases. This is consistent with higher supersaturation of the ions in the smaller amount of water at low w/c, which would increase the rate of nucleation. The nucleation rate is expected to be more sensitive to supersaturation than the growth rate [34].

Based on the analytical method suggested by Mounanga et al. [35], using the coefficients provided by Bentz et al. [36], the ratio of chemical shrinkage to degree of hydration for this composition at ambient temperature should be −0.074 ml/g, which is in excellent agreement with the measured value of −0.0764 ml/g, shown in Fig. 1. However, the constant A obtained from the BNG fits, which should represent the maximum amount of chemical shrinkage when $\alpha = 1$, is only about −0.028 ml/g, and the final measured shrinkage is about 80–95% of A, even though the final measured degree of reaction is $\alpha \approx 0.3$ to 0.5 [16]; that is, the fit implies that $\alpha \approx 0.8$–0.95 at the end of the experiment, which is twice the actual value. As shown in Table 2 [37], the Class H cement used in these experiments contains ~64 wt.% C_3S. Thus, if only the C_3S and C_3A are fully hydrated, the predicted shrinkage is −0.046 ml/g, but this is still much larger than the values of A found from the fits; the shrinkage after 48 h at 25 °C corresponds to hydration of ~60% of the C_3S. The peak in the rate of shrinkage occurs after about 6.8 h at 25 °C (see Fig. 6), when the shrinkage is −0.0061 ml/g, which is ~22% of A. Evidently, the fit forces the value of X to be large, so that extensive impingement allows the curve to match the deceleration of the reaction rate; that is, the fit falsely indicates that the hydration is nearly complete. Interestingly, Thomas et al. [38] found that nucleation and growth fits for $CaCl_2$-accelerated C_3S were better than for pure C_3S, and that the amount of early hydration that occurred during the rate peak was more than twice as great. They suggested that $CaCl_2$ increases the packing density of the initial C-S-H product, and showed SANS surface area data that support this hypothesis.

The small value of A returned by the fits could indicate a transition to diffusion control, which would mean that the fits have been applied beyond their limit of applicability. An alternative interpretation of the hydration process, recently suggested by Bishnoi and

Table 2
Mineralogical composition of Class H cement (weight %).

Component	Class H cement (OWC)[a]
C_3S	64
C_2S	16
C_3A	0.6
C_4AF	11
MgO	1.08
SO_3	2.74
K_2O	0.44
Na_2O	0.09
LoI	1.31

[a] Data from Ref. [37].

Table 3
Fitting parameters for calorimetric data from Ref. [24].

Name	Size (μm)	BET (m^2/kg)	k_G (h^{-1})	k_S (h^{-1})	O_v^{Ba} (μm^{-1})	G_2 (μm/h)	N_S (μm^{-2})
A	38.5	597.7	0.0716	0.0659	0.833	0.0859	0.187
B	82.6	376.8	0.0535	0.0616	0.525	0.102	0.116
D	17.9	1537.7	0.0916	0.0595	2.14	0.0427	0.617
E	15.4	N.A.	0.0499	0.0824	–	–	–

[a] Calculated from Eq. (22), using BET surface area, $R_{wc}=0.4$, $\rho_w=1000$ kg/m^3, $\rho_c=3150$ kg/m^3.

Scrivener [24], is that the initially formed product is extremely low in density (~1.2 g/cm^3). This material rapidly propagates through the water-filled space and later densifies by in-filling. There is some support for this from the microstructural investigation by Gallucci et al. [21]. This is an appealing idea, in that it could account for the rapid decrease in permeability in very young pastes [39]. If this is so, then the initial growth could be described by the BNG model with a factor of ϕ included in the definition of A to compensate for the volume fraction of pore solution included in the mass of hydrates; the subsequent in-filling stage would be described by a JMAK model, with nucleation distributed throughout the volume of the low-density product.

It has been suggested [29] that the low-density product could consist of a sheaf of sheets of C-S-H with pore water between then, so that the bulk density is ≤1.5 g/cm^3. If those sheaves can interpenetrate, then Eq. (23) does not apply; however, they might not interpenetrate, if the solute content of the interstitial water is too low to support growth. In that case, the propagation and impingement of those sheaves would be correctly described by the BNG model. At present, the evidence for the low-density gel is tenuous. The freeze-drying technique used by Gallucci et al. [21] can destroy a soft gel structure, owing to the stress exerted by the growth of the ice crystals [40], so one must be cautious about interpreting the microstructure of samples prepared in that way. Nevertheless, the existence of the low-density gel is clearly an important topic for future investigation.

The discrepancy in Fig. 8 between the calculated curve (based on a fit to the first 48 h of hydration) and the experimental data may indicate that hydration of another phase (or phases) becomes significant. Based on the data from Lea cited by Mounanga et al. [35], the reaction after 48 h is likely to be a combination of C_2S and C_4AF. If so, it would be necessary to add two more functions, such as Eq. (42) to describe the process. However, a similar discrepancy is observed in the fits of hydration data for pure C_3S by Thomas et al.

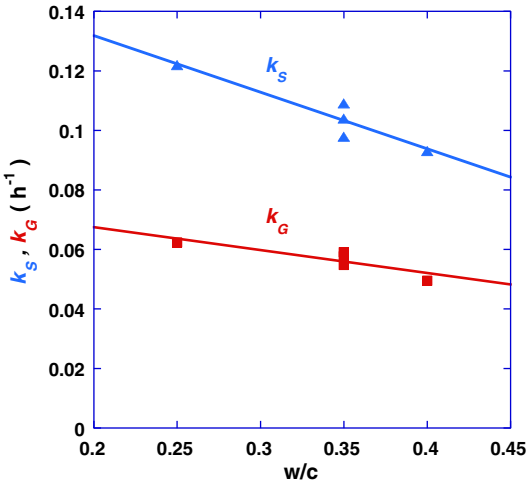

Fig. 14. Effect of water/cement ratio on constants obtained by fitting Eq. (38) to chemical shrinkage data for Class H cement.

[9,38], where no other phases are present. They attribute this to denser packing of the primary particles into space initially filled by lower density C-S-H [38]. This is similar to the picture suggested more recently by Bishnoi and Scrivener [24], except with respect to the density of the initial product.

6. Conclusions

The analysis presented here generalizes the BNG model to allow for anisotropic growth with a constant rate of nucleation or a constant number of nuclei. The latter case is more consistent with the results of detailed simulations [11]. Fitting the model to chemical shrinkage data for Class H cement [16,37] provides a very good match to the cumulative and derivative curves, and the nucleation density has the same order of magnitude found in simulations [33]. Nevertheless, the application of such models is limited to the early stages of cement hydration, when the reaction is dominated by a single phase (*viz.*, C_3S); at later times, it would be necessary to add functions describing $X(t)$ for each component that is reacting, which would require an unwieldy number of free parameters. Fortunately, for the early stage where setting of the paste occurs, this type of model is quite satisfactory. In particular, it can be used to predict the dependence of the setting time on the temperature and pressure of the reaction [41]. One must keep in mind, however, that curves of very similar shape can be obtained from models based on distinctly different physical assumptions [29], so a good fit does not prove that a given model is valid.

Acknowledgment

We are indebted to Jeffrey Bullard of NIST for helpful discussions of the hydration process, and to Shashank Bishnoi for providing calorimetric data (originally obtained by Dr. Mercedes Costoya) for hydration of alite and for enlightening discussions about the μic model.

References

[1] H.F.W. Taylor, Cement Chemistry, 2nd ed. Thomas Telford, London, 1997.
[2] E.M. Gartner, J.F. Young, D.A. Damidot, I. Javed, Hydration of Portland cement, in: J. Bensted, P. Barnes (Eds.), Structure and Performance of Cements, 2nd ed, Spon, London, 2002, pp. 57–108.
[3] J.W. Bullard, H.M. Jennings, R.A. Livingstone, A. Nonat, G.W. Scherer, J.S. Schweitzer, K.L. Scrivener, J.J. Thomas, Mechanisms of cement hydration, Cem. Concr. Res. 41 (2011) 1208–1223.
[4] J.J. Thomas, J.J. Biernacki, J.W. Bullard, S. Bishnoi, J.S. Dolado, G.W. Scherer, A. Luttge, Modeling and simulation of cement hydration kinetics and microstructure development, Cem. Concr. Res. 41 (2011) (2011) 1257–1278.
[5] P.W. Brown, J. Pommersheim, G. Frohnsdorff, A kinetic model for the hydration of tricalcium silicate, Cem. Concr. Res. 15 (1985) 35–41.
[6] S.A. FitzGerald, D.A. Neumann, J.J. Rush, D.P. Bentz, R.A. Livingston, In-situ quasielastic neutron scattering study of the hydration of tricalcium silicate, Chem. Mater. 10 (1998) 397–402.
[7] A.J. Allen, J.C. McLaughlin, D.A. Neumann, R.A. Livingston, In situ quasi-elastic scattering characterization of particle size effects on the hydration of tricalcium silicate, J. Mater. Res. 19 (11) (2004) 3242–3254.
[8] V.K. Peterson, D.A. Neumann, R.A. Livingston, Hydration of tricalcium and dicalcium silicate mixtures studied using quasielastic neutron scattering, J. Phys. Chem. B 109 (2005) 14449–14453.
[9] J.J. Thomas, A new approach to modeling the nucleation and growth kinetics of tricalcium silicate hydration, J. Am. Ceram. Soc. 90 (10) (2007) 3282–3288.
[10] J.W. Bullard, A determination of hydration mechanisms for tricalcium silicate using a kinetic cellular automaton model, J. Am. Ceram. Soc. 91 (7) (2008) 2088–2097.
[11] J.W. Bullard, R.J. Flatt, New insights into the effect of calcium hydroxide precipitation on the kinetics of tricalcium silicate hydration, J. Am. Ceram. Soc. 93 (7) (2010) 1894–1903.
[12] W.A. Johnson, R.F. Mehl, Reaction kinetics in processes of nucleation and growth, Trans. Am. Inst. Min. (Metall.) Eng. 135 (1939) 416–458.
[13] M. Avrami, Kinetics of phase change. II. Transformation–time relations for random distribution of nuclei, J. Chem. Phys. 8 (1940) 212–224.
[14] A. Kolmogorov, Statistical theory of crystallization of metals (in Russian), Akad. Nauk SSSR. Izv. Ser. Khim. (Bull. Acad. Sci. USSR. Div. Chem. Sci.), 3 (1937) 355–359.

[15] J.W. Cahn, The kinetics of grain boundary nucleated reactions, Acta Metall. 4 (1956) 449–459.
[16] J. Zhang, E.A. Weissinger, S. Peethamparan, G.W. Scherer, Early hydration and setting of oil well cement, Cem. Concr. Res. 40 (2010) 1023–1033.
[17] H.M. Jennings, Refinements to colloid model of C-S-H in cement: CM-II, Cem. Concr. Res. 38 (2008) 275–289.
[18] M. Geiker, T. Knudsen, Chemical shrinkage of Portland cement paste, Cem. Concr. Res. 12 (1982) 603–610.
[19] S. Garrault, T. Behr, A. Nonat, Formation of the C-S-H layer during early hydration of tricalcium silicate grains with different sizes, J. Phys. Chem. B 110 (2006) 270–275.
[20] J.J. Thomas, H.M. Jennings, A.J. Allen, Relationships between composition and density of tobermorite, jennite, and nanoscale $CaO–SiO_2–H_2O$, J. Phys. Chem. C 114 (2010) 7594–7601.
[21] E. Gallucci, P. Mathur, K. Scrivener, Microstructural development of early age hydration shells around cement grains, Cem. Concr. Res. 40 (2010) 4–13.
[22] A. Nonat, The structure and stoichiometry of C-S-H, Cem. Concr. Res. 34 (2004) 1521–1528.
[23] J.W. Bullard, G.W. Scherer, "C-S-H supersaturation and its effect on nucleation and growth kinetics", in preparation.
[24] S. Bishnoi, K.L. Scrivener, Studying nucleation and growth kinetics of alite hydration using μic, Cem. Concr. Res. 39 (2009) 849–860.
[25] S. Garrault, A. Nonat, Hydrated layer formation on tricalcium and dicalcium silicate surfaces: experimental study and numerical simulations, Langmuir 17 (2001) 8131–8138.
[26] D.P. Birnie III, M.C. Weinberg, Kinetics of transformation for anisotropic particles including shielding effects, J. Chem. Phys. 103 (9) (1995) 3742–3746.
[27] J.W. Cahn, The time cone method for nucleation and growth kinetics on a finite domain, Mater. Res. Soc. Symp. Proc. 398 (1996) 425–437.
[28] E. Villa, P.R. Rios, Transformation kinetics for surface and bulk nucleation, Acta Mater. 58 (2010) 2752–2768.
[29] G.W. Scherer, "Models of confined growth", submitted to Cem. Concr. Res.
[30] T. Kasuya, K. Ichikawa, M. Fuji, H.K.D.H. Bhadeshia, Real and extended volumes in simultaneous transformations, Mater. Sci. Technol. 15 (1999) 471–473.
[31] D. Damidot, A. Nonat, P. Barlet, Kinetics of tricalcium silicate hydration in diluted suspensions by microcalorimetric measurements, J. Am. Ceram. Soc. 73 (11) (1990) 3319–3322.
[32] J.J. Thomas, "The instantaneous apparent activation energy of cement hydration measured by a novel calorimetry-based method", submitted to J. Am. Ceram. Soc.
[33] J.W. Bullard, private communication.
[34] J.W. Christian, The Theory of Transformations in Metals and Alloys, Part I, Pergamon, New York, 1975.
[35] P. Mounanga, A. Khelidj, A. Loukili, V. Baroghel-Bouny, Predicting $Ca(OH)_2$ content and chemical shrinkage of hydrating cement pastes using analytical approach, Cem. Concr. Res. 34 (2004) 255–265.
[36] D.P. Bentz, P. Lura, J.W. Roberts, Mixture proportioning for internal curing, Concrete International, February 2005, pp. 35–40, See also, http://ciks.cbt.nist.gov/bentz/Mixpropfin/node2.html.
[37] S. Peethamparan, E. Weissinger, J. Vocaturo, J. Zhang, G. Scherer, Monitoring chemical shrinkage using pressure sensors, ACI Special Proceedings in CD on Advances in the Material Science of Concrete, SP-270, 2010, pp. 77–88.
[38] W. Vichit-Vadakan, G.W. Scherer, Measuring permeability and stress relaxation of young cement paste by beam-bending, Cem. Concr. Res. 33 (2003) 1925–1932.
[39] G.W. Scherer, Freezing gels, J. Non-Cryst. Solids 155 (1993) 1–25.
[40] J.J. Thomas, A.J. Allen, H.M. Jennings, Hydration kinetics and microstructure development of normal and $CaCl_2$-accelerated tricalcium silicate pastes, J. Phys. Chem. C 113 (2009) 19836–19844.
[41] G.W. Scherer, G.P. Funkhouser, S. Peethamparan, Effect of pressure on early hydration of class H and white cement, Cem. Concr. Res. 40 (2010) 845–850.